IN-PLANE PERMEABILITY OF ORIENTED STRAND LUMBER, PART I: THE EFFECTS OF MAT DENSITY AND FLOW DIRECTION

Chao Zhang
Graduate Research Assistant

*Gregory D. Smith**†
Associate Professor
Department of Wood Science
University of British Columbia
Vancouver, BC, Canada V6T 1Z4

(Received June 2009)

Abstract. The in-plane permeability was measured for thick, unidirectional oriented strand lumber made from aspen (*Populus tremuloides*) strands and pressed to five different densities. The press cycle was such that the vertical density profile of the panels was uniform. Specimens were cut from the boards and sealed inside a specially designed specimen holder; this jig was connected to a permeability measurement apparatus and in-plane permeability measured parallel, perpendicular, and 45° to the strand orientation. Permeability decreased markedly with increasing board density. The highest permeability was in the strand alignment direction and lowest perpendicular to it. The permeability in the 45° direction fell between those in parallel and perpendicular to strand alignment. A polynomial equation was fit to the results of each direction with r^2 of 0.938 and 0.993. The in-plane distribution of permeability as a function of flow direction was obtained and its vector diagram was lenticular in shape.

Keywords: Oriented strand lumber, wood composites, in-plane permeability, density, flow direction.

INTRODUCTION

Oriented strand board (OSB) and oriented strand lumber (OSL) are widely used in residential construction. Data on OSL production volumes are very difficult to find because these data are commonly aggregated with OSB production volumes or with structural composite lumber volumes (eg glulam, laminated veneer lumber, parallel strand lumber, and so on). Although the annual production volume of OSL is much smaller than that of OSB, it is presumed that because of their similar raw material inputs and manufacturing processes, trends in OSB market volumes are a reasonable indicator of production trends for OSL. In 2007, the production of OSB in North America was 21.2 Mm^3 accounting for 59% of the structural panel market (UNECE 2009). However, in 2008 with the US housing collapse and the ensuing financial crisis, the OSB production fell to 18.0 Mm^3, was forecast to drop to 17.7 Mm^3 for 2009 (UNECE 2009), and will likely remain low throughout 2010 (RISI 2008). Panel manufacturers have also had to face increasing costs for nearly all inputs (wood, resins, energy, and labor) combined with a shrinking market and stronger competition from overseas companies. Therefore, there is considerable need to improve production efficiency in OSB plants and by extension in OSL plants.

Hot-pressing is one of the most important processes in the manufacture of strand-based wood composites and is often the production-limiting step in a plant. During the press cycle, a loosely formed strand mat is subjected to high temperature and pressure and is pressed to its target thickness. Once the mat comes into contact with the platens, heat flows into the strands and steam is formed, which increases the internal gas pressure within the mat. If the gas cannot escape from the

* Corresponding author: greg.smith@ubc.ca
† SWST member

panel, this high internal gas pressure can result in a catastrophic delamination or "blow" and the whole panel may be lost. Obviously, this is to be avoided. Careful control of mat permeability and the associated changes in void structure during the press cycle should reduce the likelihood of blown panels and increase the overall throughput and profitability of the plant.

Early research on void structure in wood composites included Suchsland (1959), who developed a model that related flake shape and alignment to void distribution. Haas et al (1998) measured the in-plane and transverse permeability of OSB pressed to different densities with resin contents of 5 and 11%. The results were fitted to empirical equations as a function of mat density. They found the in-plane permeability to be about 10 times that in transverse direction, whereas the in-plane permeability in parallel and perpendicular directions were of the same order of magnitude. Garcia et al (2001) investigated internal temperature and gas pressure during hot-pressing and found that for OSB, increasing panel density reduced permeability (both lateral and transverse) and increasing flake alignment increased in-plane permeability. Hood (2004) and Hood et al (2005) examined the effects of flake thickness and mat density of OSB on gas permeability through transverse and in-plane directions of the mats. No adhesive was used in the formation of the mats with the exception of the highest density (800 kg/m^3) panels. Both transverse and in-plane permeability decreased rapidly as the compaction ratio increased; transverse and in-plane permeability was higher for mats composed of thicker flakes. Empirical equations were also developed for three principal directions. Dai et al (2005) developed a model for transverse permeability based on the Carman-Kozeny theory and the mat structure, which linked mat permeability to mat porosity and strand dimensions. Fakhri et al (2006a, 2006b) examined the effects of density and core fines content on the transverse permeability of OSB. The core permeability decreased with increasing density and it increased exponentially with fine content from 0 – 75% at each density level.

Although in-plane flow is the main path for gas escape during hot-pressing of strand-based panels (Haas et al 1998; Hood et al 2005), little work to date has addressed the in-plane permeability of OSL, and the in-plane permeability distribution has not been reported in the literature. This work aims to fill this gap and provide permeability data to aid potential process improvement in industry. It was also preliminary work for the development of OSL products from mountain pine beetle-killed wood (MPB-OSL). The results of this study will be combined with a future permeability investigation that is expected to help the industry efficiently switch from processing conventional OSL to MPB-OSL.

The objective was to investigate the effects of gas flow direction and board density on the in-plane permeability of OSL. A methodology was developed to measure in-plane permeability on relatively large-scale specimens (samples longer than strand length). Empirical equations were then derived to predict the in-plane permeability parallel (0°), perpendicular (90°), and 45° to the strand alignment direction. Finally, the in-plane distribution of permeability was described in a vector diagram.

MATERIALS AND METHODS

Experimental Design

The two factors examined in this study were panel density and flow direction (with strand alignment). The five densities were 450, 550, 625, 700, and 800 kg/m^3. Four replicates were made for each density for a total of 20 OSL panels. The in-plane permeability of each board was measured in 0, 90, and 45° directions. To avoid confounding effects from density gradients through the sample thickness, the panels were pressed such that a uniform vertical density profile (VDP) was obtained.

Board Manufacture

Aspen (*Populus tremuloides*) strands (supplied by Ainsworth Lumber Co Ltd, Grande Prairie,

AB) were 150 to 180 mm long, 25 mm wide, and 1 mm thick. The resin used was Cascophen OSF-59FLM, a liquid phenol–formaldehyde resin with a solids content of 59%. The resin content was 6% based on the oven-dried weight of the strands and no wax was used to minimize the confounding effects from its presence. The panels were designed to have a 559 mm length, 305 mm width, and 31.8 mm thickness.

The strands and resin for a board was mixed in a 1.5 m dia by 0.6 m deep drum blender. The blender was loaded with strands for one panel only. Resin was atomized using compressed air and sprayed onto the strands in 180 – 240 s and the blender was left rotating for another 420 s. The blended strands were hand-sorted and strands with lengths of 100 – 180 mm and widths of 20 – 40 mm were selected; broken strands and fine materials were discarded. The mat was hand-formed to ensure a unidirectional strand alignment and uniform horizontal mass distribution. A set of 15 preliminary panels was made to determine a press cycle for producing a uniform VDP and to ensure that the boards reached the target density range.

The press cycle was as follows: the platens were preheated to 50°C, the mat was placed onto the lower press platen, and the press closed using displacement control at a rate of 4 mm/s over 12 s to the final thickness. This position was maintained for 40 min while the platens were heated to 200°C (time from 50 – 200°C was approximately 20 min). A short degas period was not used for panels with densities below 800 kg/m^3 because the core gas pressure after 40 min was low (below 20 kPa). The press was then opened at 25 mm/s. The 800 kg/m^3 panels behaved very differently from the other panels and blew the moment the press was opened (core gas pressure was approximately 850 kPa). A 60 s degas period was added to the press cycle but the boards continued to blow. Finally, the pressing time was increased to 70 min and the platen temperature reduced to 180°C (to reduce browning of the panel surfaces) and no further blows occurred. The closing time and closing speed were not changed for 800 kg/m^3 to keep these parameters consistent for all panels.

Sample Preparation and Vertical Density Profile Measurements

One permeability sample measuring 203 × 203 mm and 8 VDP samples measuring 51 × 51 mm were cut from each panel. The cutting pattern (Fig 1) was the same for all panels. The samples were conditioned at 20°C and 65% RH for at least 15 days before testing. The VDP measurements were performed using the Quintek Measurement System (Model QDP-01X) and the results recorded by the QMS Density Profile System, Version 1.30.

Measurement of In-Plane Permeability

Specimen holders were designed and fabricated to measure the in-plane permeability of OSL samples. Its purpose was to seal four of the six sample faces to force air to flow in the desired direction. The two free sample ends were connected to a permeability measurement apparatus. The specimen holders consisted of six aluminum plates: top and bottom face plates, two side plates, and two end plates (Fig 2). Two different sets were designed to perform the measurements in three directions: one 203 mm wide for 0° and 90° measurements and one 127 mm wide for the 45° measurement. Holes were drilled on the two end plates to be connected to the permeability measurement apparatus.

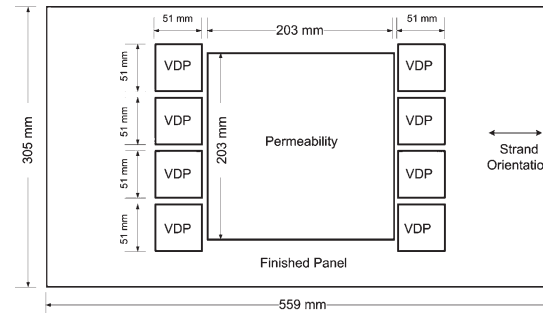

Figure 1. Cutting patterns for permeability specimens and vertical density profile specimens.

Hot-melt was found to be the most appropriate glue that met the sealing requirements and the repetitive assembly and disassembly of the specimen holder; the complete details for other glues tried were reported by Zhang (2009). Sealing between the surfaces of plates and specimens on a cross-section is shown in Fig 3. The hot-melt used was Scotch-Weld 3738AE with a 54°C adhesive failing point and 86°C melting point. Once a specimen had been sealed in the specimen holder and cooled to room temperature, it was connected to a permeability measurement apparatus designed according to the theory of Siau (1995). It was capable of measuring the specific permeability of $10^{-16} - 10^{-10}$ m^3/m.

To determine if the hot melt assembly process was adequate to ensure that all air pathways around the specimen had been blocked, a test with an impermeable, solid acrylic sample of the same dimensions as the OSL samples was prepared. After being connected to the permeability apparatus, it was found that the water level remained constant indicating no gas flow and that an airtight seal had been achieved. It is noteworthy that almost all of the hot-melt glue stayed on the OSL specimen surfaces; inspection with a hand lens of cross-sections cut from preliminary samples showed that the penetration was minimal (<0.1 mm).

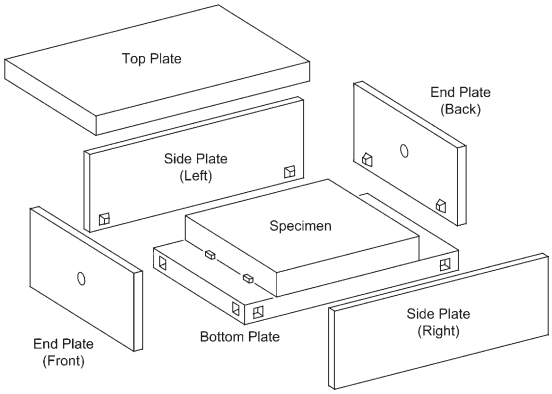

Figure 2. Design of the specimen holder for permeability measurement.

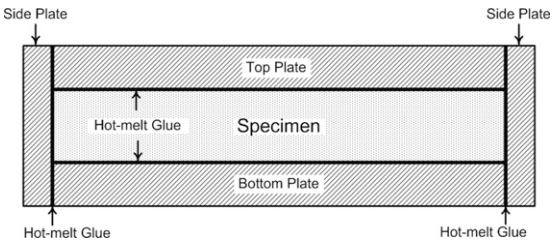

Figure 3. Cross-sectional view of the specimen holder plates sealed with hot-melt glue.

Superficial permeability was calculated by Darcy's law (Siau 1995) and then converted to specific permeability, which is independent of the measuring fluid.

$$K = k\eta \qquad (1)$$

where η is the dynamic viscosity (Pa/s), k is the superficial permeability ($m^2 \cdot Pa^{-1} \cdot s^{-1}$), and K is the specific permeability (m^3/m). A dynamic viscosity value of 1.846×10^{-5} Pa·s was used for standard air at 25°C.

The permeability of the samples in the 0° direction was measured first. The two sealed sides of the specimen were then trimmed off to produce a clean cross-section for a subsequent test in the 90° direction. Finally, a 127 × 127 mm specimen was cut along a direction at 45° to the strand alignment. This sequence is shown schematically in Fig 4.

Statistical Analysis

The results were entered into an Excel spreadsheet and the permeability computed. The data were imported into MINITAB software

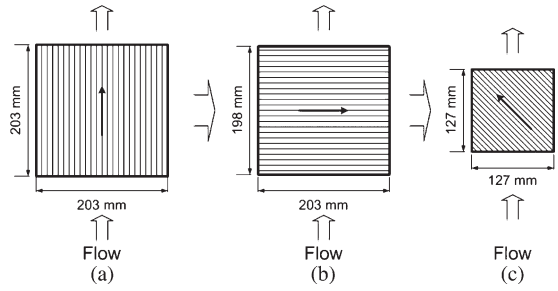

Figure 4. Specimen cutting sequences and specimen dimensions for three gas flow directions: (a) 0°, (b) 90°, and (c) 45°. The arrows in the specimens indicate the directions of strand alignment.

(Version 15.1.1.0) and analysis of variance (ANOVA) performed using a significance level of $\alpha = 0.05$. Significant differences between density levels were identified using Tukey's Honestly Significant Difference (HSD) test. An empirical equation was developed by performing regressions on the data obtained in each direction and r^2 values for the computed fits.

RESULTS AND DISCUSSION

Vertical Density Profile

The VDPs for typical specimens of each density level are shown in Fig 5. It indicates that panels had reasonably uniform VDPs and were not a combination of core and surface layers of different densities.

Effect of Density on In-Plane Permeability

The original permeability data were not normally distributed ($p < 0.01$), and a logarithmic transformation was applied. The transformed permeability was found to be normally distributed ($p > 0.05$). All of the statistical analyses described subsequently were performed on the transformed data. The mean and standard deviation of the sample densities are listed in Table 1. The density was oven-dry because MC effects were not within the scope of the research.

The permeability measured for each board is plotted as a function of density in Fig 6. The ANOVA revealed that density had a significant effect on permeability in each direction ($p < 0.001$). Tukey's HSD test indicated that the permeability difference between any two density levels was significant for all directions with the exception of the 625 and 700 kg/m^3 samples in the 45° direction.

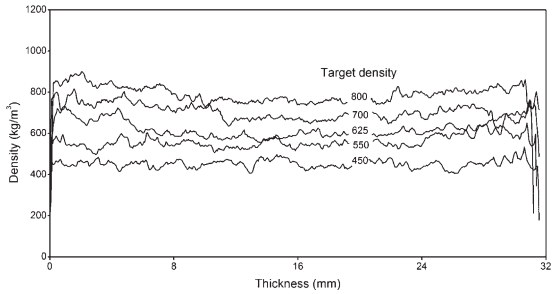

Figure 5. Vertical density profile of specimens with different target densities.

Table 1. *Average density of permeability and vertical density profile (VDP) specimens for each density level.*[a]

Samples	Replicates	Density level (kg/m^3) 450	550	625	700	800
Permeability	4	442 (6.8)	537 (4.3)	598 (6.8)	668 (5.3)	797 (13.9)
VDP	32	445 (19.4)	542 (21.6)	608 (16.5)	678 (20.8)	781 (31.1)

[a] Standard deviation given in parentheses.

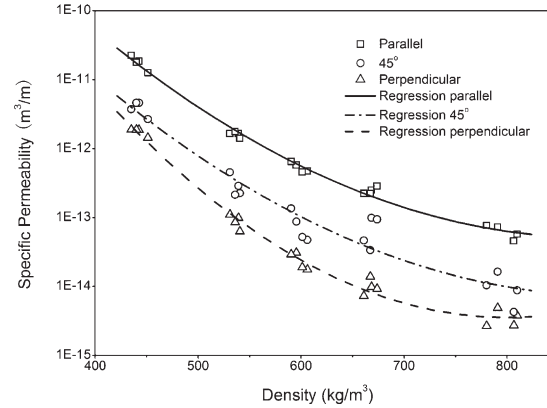

Figure 6. Comparison of specific permeability values in different directions with polynomial regression lines.

Because a linear regression performed in each direction yielded unequal variances, a second-order polynomial regression was conducted to arrive at the empirical equations as follows:

$$\log(K_0) = -3.285 - 0.02261 \times \rho + 1.277 \times 10^{-5} \times \rho^2 \quad (r^2 = 0.993) \tag{2}$$

$$\log(K_{45}) = -3.944 - 0.02258 \times \rho + 1.250 \times 10^{-5} \times \rho^2 \quad (r^2 = 0.938) \tag{3}$$

$$\log(K_{90}) = -1.122 - 0.03333 \times \rho + 2.084 \times 10^{-5} \times \rho^2 \quad (r^2 = 0.988) \tag{4}$$

where K_0, K_{90}, and K_{45} are specific permeability (m^3/m), in which the subscripts indicate the

angle between flow direction and strand alignment (in degrees), and ρ is oven-dry panel density (kg/m^3).These regression lines are compared with the original data in Fig 6 from which one can conclude that Eqs 2 to 4 are reasonable descriptions of the data.

An inverse relationship between permeability and density is what one would intuitively expect; because the void space between the particles decreases and the interconnections between adjacent voids is reduced, it becomes more difficult for air to move through the material. Dai et al (2005) found that samples made from longer, thinner strands had lower permeability than those made from shorter, thicker strands, a finding similar to that of Hood et al (2005) who reported that permeability decreased with decreasing strand thickness. The in-plane permeability of OSB samples reported by Hood et al (2005), who used strands 100 mm long, 25 mm wide, and 1.0 mm thick, were of the same order of magnitude as this work but differed in the change with density; their samples were more permeable than ours for densities below 720 kg/m^3 and less permeable above it. Because Hood et al (2005) used different wood species, resin content, and strand sizes than in this study, the difference in slope is likely from these differences. Haas et al (1998) reported slightly higher permeability than found in this study for the same density. The reason for the difference may be from the thinner strands (0.6 mm thick) used by Haas et al (1998) compared with the thicker strands used in this work (1.0 mm thick).

Dai and Steiner (1993) noted that gas flow in strand-based composites can be divided into two types: interstrand, referring to flow through voids between strands, and intrastrand, referring to flow within strands. Bolton and Humphrey (1994) hypothesized that flow in the mat was dominated by interstrand voids. Dai et al (2005) proved this hypothesis for transverse permeability of strand-based panels by comparing the transverse permeability of aspen OSB with the perpendicular-to-grain permeability of aspen wood compressed to the same density.

Whether the hypothesis is true for in-plane permeability is unclear. According to Avramidis and Mansfield (2005), the longitudinal permeability of aspen was 22.94 $\times$ 10^{-10} m^3/m for sapwood and 1.95 $\times$ 10^{-10} m^3/m for heartwood, both of which were higher than the in-plane permeability (0° direction) of OSL at the same density. However, because the longitudinal permeability of densified aspen wood was not presently available, it was not possible to compare the permeability in the same way as done by Dai et al (2005).

Effect of Flow Direction on In-Plane Permeability

The permeability in each flow direction and board density is shown in Fig 6. Permeability was the highest in the 0° direction and lowest in the 90° direction; values for the 45° direction lay between these and had a higher variability at each density than the other directions.

The ratios of K_{90}/K_0 and K_{45}/K_0 provide a measure of the anisotropy of in-plane permeability, as shown in Fig 7. K_{90}/K_0 was less than 0.12 over the entire density range. This ratio decreased with density increasing to 700 kg/m^3, after which it increased slightly. The ratio of K_{45}/K_0 was more variable and there was a slight downward trend with increasing density, but it was not significant for the number of specimens tested. The permeability in the 0° direction was

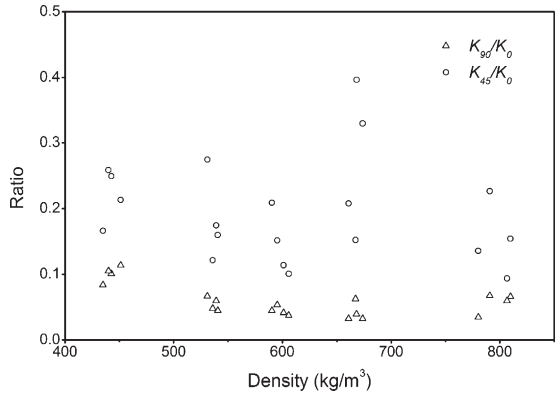

Figure 7. Ratio of permeability values in different directions representing the permeability anisotropy of the panels.

10 – 30 times greater than that in the 90° direction. Note the two points at the 700 kg/m^3 level that were much higher than other values. The cause of this is uncertain but could be the result of some strands not being unidirectionally oriented during forming.

A relationship for the ratio K_θ/K_0 (denoted as K_r) as a function of the gas flow direction θ between 0 – 90° was obtained by performing a second-order polynomial curve fit to the data. Eq 5 was obtained with an r^2 of 0.931. It is important to point out that the curve fit was to the raw permeability data results and not to the mean results for each angle. Such a high r^2 value is not surprising because permeability was only measured in three directions; had there been sufficient time and resources to measure flow in more directions, the r^2 value may well be lower.

$$K_r = K_\theta/K_0 = 0.7693 \times (\sin\theta)^2 - 1.709 \times \sin\theta + 1.000 \quad (5)$$

where K_θ is the specific permeability in a direction with angle θ to the strand alignment and K_0 is the specific permeability in the 0° direction.

The change in magnitude of normalized K with direction θ is shown in Fig 8, in which the vector connecting O and Point P in the $\overrightarrow{OP}(K_r, \theta)$ curve indicates the permeability in that direction. As one would expect, the curve is symmetric about the 0° and 90° directions with each lobe being lenticular in shape.

Because permeability is flux divided by pressure gradient according to Darcy's law, flux is proportional to permeability under the same pressure gradient. Therefore, Fig 8 also shows the relative flux distribution at point (0, 0). Similar to permeability, relative flux is the ratio of flux at angle θ and that of the parallel-to-strand direction.

$$F_r(\theta) = 0.7693 \times (\sin\theta)^2 - 1.709 \times \sin\theta + 1.000 \quad (6)$$

The flux between angles 0° and θ can be calculated by the area between $F_r(\theta_1)$ and $F_r(\theta_2)$:

$$F_r(\theta_1, \theta_2) = \int_{\theta_1}^{\theta_2} \frac{1}{2}[F_r(\theta)]^2 d\theta = 1.73\theta + 2.70\cos\theta - 0.11\cos\theta - 0.63\sin(2\theta) + 0.0092\sin(4\theta)\Big|_{\theta_1}^{\theta_2} \quad (7)$$

A standardized cumulative percentile curve can be plotted as shown in Fig 9, in which the point represents the percentage of flux flowing between 0° and θ. Because the curve in Fig 8 is symmetric in both horizontal and vertical axes, only one fourth from 0° to 90° is shown in Fig 9. It indicates that for an in-plane circular area around center O per unit time, more than 50% of the air flows in a narrow area between 0° and 10° and more than 90% of the air flows between 0° and 30°.

The interpretation of the physical status of flow paths could provide some explanation of the trend obtained: unidirectionally oriented strands created small, narrow paths for air along the sides of strands (interstrand voids) through which gases flowed in the 0° direction; vessels in aspen (intrastrand voids) were connected by a single opening occupying almost the whole perforation plate (Hoadley 1990), so they could provide long

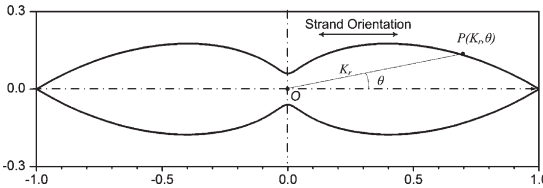

Figure 8. The in-plane distribution of specific permeability at point O.

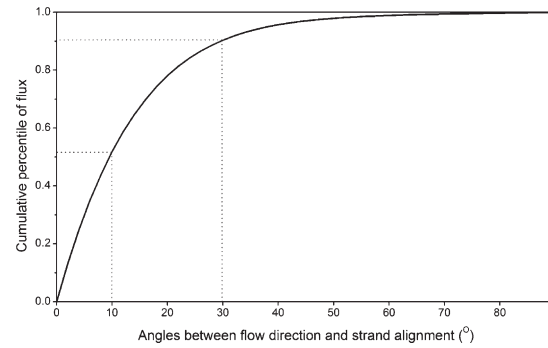

Figure 9. Cumulative flux curve from 0° to 90°.

and interconnected channels for gas to flow through. However, when air was forced in the 90° direction, the flow was also perpendicular to the interstrand and intrastrand paths and it had to pass through numerous layers of strands and cell walls. Therefore, gas flow in the perpendicular direction was considerably less than that in the parallel direction. In the case of an angle between 0° and 90° to strand orientation, the air flowed through the mat in a tortuous combination of parallel and perpendicular paths; thus, the permeability values fell between the 0° and 90° results.

CONCLUSIONS

1. The specimen holders designed for in-plane permeability measurements of wood composites were found to be capable of sealing samples well and restricting the gas flow to the desired direction.
2. Both density and flow direction had significant effects on the in-plane permeability of OSL. Permeability decreased markedly as the density increased. Permeability was highest in the 0° direction and lowest in the 90° direction. The permeability in the 45° direction had higher variability and its magnitude fell between that of the 0° and 90° directions.
3. There was a second-order polynomial relationship between $\log_{10}$ transformed permeability and the board density. The empirical equations agreed with experimental results well with an r^2 above 0.93.
4. The permeability in the 0° direction was 10 – 30 times greater than that in the 90° direction. The in-plane permeability distribution was obtained and had a symmetric lenticular shape. The cumulative curve indicated that 50% of the gas flowed through a circular sector area between 0° and 10°, and 90% of the gas flowed between 0° and 30°.

ACKNOWLEDGMENTS

The financial support from Forestry Innovation Investment Ltd is greatly appreciated. A special thanks to Ainsworth Lumber Canada Ltd for providing the strands, to Hexion Canada for the PF resin, and to Forintek Canada Corp (Vancouver) for the use of their facilities. We thank Dr. S. Avramidis for kindly providing permeability measuring apparatus and guidance. Thanks are also extended to Dr. Kate Semple, Department of Wood Science, for comments on the manuscript.

REFERENCES

Avramidis S, Mansfield SD (2005) On some physical properties of six aspen clones. Holzforschung 59(1):54 – 58.

Bolton AJ, Humphrey PE (1994) The permeability of wood-based composite materials. Part 1. A review of the literature and some unpublished work. Holzforschung 48(Suppl):95 – 100.

Dai C, Steiner PR (1993) Compression behaviour of randomly-formed wood flake mats. Wood Fiber Sci 25(4):349 – 358.

Dai C, Yu C, Zhou X (2005) Heat and mass transfer in wood composite panels during hot pressing: Part II. Modeling void formation and mat permeability. Wood Fiber Sci 37(2):242 – 257.

Fakhri H, Semple K, Smith G (2006a) Permeability of OSB. Part I. The effects of core fines content and mat density on transverse permeability. Wood Fiber Sci 38(3):450 – 462.

Fakhri H, Semple K, Smith G (2006b) Transverse permeability of OSB. Part II. Modeling the effects of density and core fines content. Wood Fiber Sci 38(3):463 – 473.

Garcia PJ, Avramidis S, Lam F (2001) Internal temperature and pressure responses to flake alignment during hot-pressing. Holz Roh Werkst 59(4):272 – 275.

Haas G, Steffen A, Fruhwald A (1998) Permeability of fiber, particle, and strand mats to gas. Holz Roh Werkst 56(6):386 – 392.

Hoadley BR (1990) Understanding wood: accurate results with simple tools. Taunton Press, Newton, MA. 280 pp.

Hood JP (2004) Changes in oriented strandboard permeability during hot-pressing. MS thesis, Virginia Polytechnic Institute, Blacksburg, VA. 85 pp.

Hood JP, Kamke FA, Fuller J (2005) Permeability of oriented strandboard mats. Forest Prod J 55(12):194 – 199.

RISI (2008) North American wood panels forecast (December). RISI, Boston, MA.

Siau JF (1995) Wood: Influence of moisture on physical properties. Department of Wood Science and Forest Products, Virginia Polytechnic Institute and State University, Blacksburg, VA. 227 pp.

Suchsland O (1959) An analysis of the particle board process. Michigan Quarterly Bulletin 42(2):350 – 372.

UNECE (2009) Timber Committee Market Statement on forest products markets in 2008 and 2009. United Nations Economic Commission for Europe, Geneva, Switzerland.

Zhang C (2009) Measurement and modeling of the in-plane permeability of oriented strand-based wood composites. MSc thesis, University of British Columbia, Vancouver, Canada. 89 pp.